Title	Direct evidence for decomposition of antigorite under shock loading
Auther(s)	Sekine, Toshimori; Meng, Chuanmin; Zhu, Wenjun; He, Hongliang
Citation	Journal of Geophysical Research - Solid Earth , 117 : B03212
Issue Date	2012
DOI	10.1029/2011JB008439
Self DOI	
URL	http://ir.lib.hiroshima-u.ac.jp/00034742
Right	(c) 2012 by the American Geophysical Union.
Relation	

Direct evidence for decomposition of antigorite under shock loading

Toshimori Sekine,[1] Chuanmin Meng,[2] Wenjun Zhu,[2] and Hongliang He[2]

Received 11 April 2011; revised 18 January 2012; accepted 27 January 2012; published 23 March 2012.

[1] Detailed wave profiles of antigorite (a serpentine mineral) under plate-impact shock loading have been measured to a pressure of 131 GPa in order to understand its dynamic behavior because serpentine is present in pristine meteorites as well as in the Earth mantle. All the profiles indicate single wave structures, and a sudden decrease in density was detected at ~60 GPa with increasing pressure when shock-loaded for a long duration (~0.6 μs) using a thick flyer. Such a drop in density also was observed during recompression by a high-impedance window material (LiF). Although exothermic decomposition is generally considered to be fast, the decomposition of antigorite under shock loading requires a reaction time so that the Hugoniot may represent a metastable state at which stable phase cannot appear in a timely way. Based on these observations, antigorite decomposes exothermically into an assemblage of either brucite + stishovite + periclase or brucite + perovskite above a shock pressure of 60 GPa, but does not dehydrate endothermically into assemblages with water fluid. The observed dynamic behavior of serpentine, coupled with the previous results of the shock-recovered serpentines, reinforces that serpentine plays a key role to carry water within the snowline of the solar system.

Citation: Sekine, T., C. Meng, W. Zhu, and H. He (2012), Direct evidence for decomposition of antigorite under shock loading, *J. Geophys. Res.*, *117*, B03212, doi:10.1029/2011JB008439.

1. Introduction

[2] Because serpentine (chrysotile) occurs in fine-grained chondrites and has been thought to play an important role to be a possible carrier of water during planetary formation [e.g., *Lauretta et al.*, 2000; *Ciesla et al.*, 2003; *Brearly*, 2006], and because serpentine (antigorite) dehydrates in the subducted oceanic lithosphere at depth around 150–250 km [e.g., *Dobson et al.*, 2002], it is important to know the dynamic behaviors of serpentine under high pressure conditions. Serpentines with a general formula $Mg_3Si_2O_5(OH)_4$ are hydrous phyllosilicates formed during hydrothermal alternation or hydration of anhydrous Fe-Mg minerals. Antigorite is one of the three basic serpentine forms; lizardite, chrysotile, and antigorite, and is stable at high pressure and high temperature although its high Al_2O_3 content may enhance its stability [*Bromiley and Pawley*, 2003]. Many experimental studies on serpentines, including antigorite, have been carried out as well as theoretical investigations to understand the dehydration and phase transformation [e.g., *Irifune et al.*, 1996; *Stalder and Ulmer*, 2001], elastic properties [e.g., *Katayama et al.*, 2009; *Mookherjee and Stixrude*, 2009; *Bezacier et al.*, 2010; *Christensen*, 2004; *Schmitt et al.*, 2007], and mechanical properties [e.g., *Jung et al.*, 2009].

[3] Shock wave studies can provide the equation of state of minerals and dynamic behaviors at high pressures. The Hugoniots of serpentine and serpentinized rock have been determined to a shock pressure of 150 GPa [*Marsh*, 1980; *Tyburczy et al.*, 1991]. They indicate that the measured shock velocity (Us) and particle velocity (Up) relations are approximated by two lines up to a pressure of 100 GPa; the compressible low-pressure phase below 40 GPa and the high-pressure phase above 40 GPa. Above 125 GPa, there seems to be another high-pressure phase [*Tyburczy et al.*, 1991]. On the other hand, hydrous phases such as brucite [*Simakov et al.*, 1974; *Duffy et al.*, 1991] and muscovite [*Sekine et al.*, 1991] of which Hugoniots have been determined experimentally display almost linear Us-Up relations up to the maximum pressures over 100 GPa with no distinct change in the pressure-density relations. This means that the volume changes associated with phase transformations are considerably small in the two hydrous minerals of brucite and muscovite if any, but serpentine behaves differently. In order to observe the phase transition of serpentine (antigorite) by shock compression directly, we measured wave profiles for antigorite with a high time resolution. These profiles will be useful to identify the Hugoniot and the released state from the Hugoniot, and will provide information related to the dynamic behavior of serpentine (antigorite) which differs significantly from those of brucite and muscovite.

[4] Here we present evidence that antigorite decomposes through an exothermic reaction based on the Hugoniot

[1]Department of Earth and Planetary Systems Science, Hiroshima University, Higashi-Hiroshima, Japan.
[2]National Key Laboratory of Shock Wave and Detonation Physics, Institute of Fluid Physics, Chinese Academy of Engineering Physics, Mianyang, China.

0148-0227/12/2011JB008439

Table 1. Chemical Composition of Serpentine[a]

	Antigorite	Lizardite
SiO_2	43.56	42.28
TiO_2	-	0 .04
Al_2O_3	1.86	0.42
Cr_2O_3	0.11	-
CaO	-	0.03
MgO	41.09	41.94
FeO	1.65	0.36
NiO	0.1	-
MnO	-	0.08
Fe_2O_3	1.52	-
K_2O	-	0.02
Na_2O	-	0.01
H_2O	11.92	12.7
Total	101.82	97.88

[a]Compositions are in wt%. Antigorite and lizardite were used in the present study and by *Tyburczy et al.* [1991], respectively. The composition of antigorite is cited after *Uehara and Shirozu* [1985].

measurements. Antigorite is expected to have a high stability against impact, and this confirms that antigorite can be a potential candidate of water carrier in the accretion process of the solar system.

2. Experimental Procedures

[5] We used a natural antigorite (about 50 mm × 50 mm × 100 mm) from Nakanochaya, Miyazu city, Kyoto prefecture, Japan. The cell parameters are $a = 0.5446$ nm, $b = 0.9250$ nm, $c = 0.7260$ nm, and $\beta = 91.45°$ [*Uehara and Shirozu*, 1985]. The bulk chemical composition [*Uehara and Shirozu*, 1985] is listed in Table 1 and compared with that of lizardite investigated by *Tyburczy et al.* [1991]. We measured the density of each sample (∼20 mm × 20 mm × 2.5 mm) by Archimedean method. It ranges between 2.606 and 2.638 g/cm^3. The calculated density of antigorite is 2.62 ± 0.01 g/cm^3 based on the x-ray diffraction data [*Bezacier et al.*, 2010], indicating that our sample has little porosity.

[6] Planar impact experiments were carried out using a two-stage light gas gun at Institute of Fluid Physics (IFP), China, and a 30 mm-bore propellant gun at National Institute for Materials Science (NIMS), Japan. Figure 1 illustrates the target assemblage. In each shot, the impact velocity of the projectile and the particle velocity at the mirror (∼10 μm thick Al foil) sandwiched between sample and LiF window were measured using interferometers; a displacement interferometer system for any reflector (DISAR) at IFP, China [*Weng et al.*, 2006, 2008; *Jensen et al.*, 2007], and a velocity interferometer system for any reflector (VISAR) at NIMS, Japan [*Barker and Hollenbach*, 1972; *Sekine et al.*, 2008]. The LiF window remains transparent during the shock process and the interface particle velocity in the both experiments was monitored in a time-resolved way. The density of antigorite is close to that of LiF, and the Up and pressure of antigorite should be similar to those of LiF. We carried out seven shots, and in four of them we measured the Us simultaneously by the six-pins method. Each pin was located around and on the sample at 60 degree apart, as illustrated in Figure 1. These pins give us the arrival time of shock wave at each point. Based on these four data, we introduced linking factors, as explained in next section, in order to estimate Up and pressure for antigorite from the measured Up for LiF in the other three shots. The calculated Up and pressure are listed together in Table 2. The pressure range is 20 GPa to 130 GPa, which is similar to that of lizardite [*Tyburczy et al.*, 1991].

3. Experimental Results

[7] Figure 2 shows the measured wave profiles. The steady velocity is read directly as the measured Up of LiF in Table 2. For LiF, the relationship of Us (km/s) = 5.15 + 1.35Up (km/s) [*Marsh*, 1980] is used to calculate Us, and pressure P is calculated as $P = \rho_0 UsUp$ where ρ_0 is the initial density of sample. The steady velocity lasts until the shock wave is overtaken by a rarefaction wave and this time depends on the thickness of flyer plate and the impact conditions. Parts of the wave profiles after the rarefaction wave arrival show distinct features dependent on the final pressure and the compression duration. The longer the compression, the shallower the release wave profiles appear as shown by arrows in Figure 2 (shots 7 and 1). The higher the peak shock pressure, the more pronounced the plastic behavior that can be seen (shots 3 and 2) once release wave arrives. In these shots, a steady velocity on the release appears to be 2.00 km/s (shot 3) and 2.42 km/s (shot 2).

[8] Table 2 lists the experimental results on antigorite as well as LiF. The Us-Up relations for the flyer materials were employed from the Hugoniot data [*Marsh*, 1980]. As listed in Table 2, the measured Up of LiF is significantly smaller than that of antigorite that was calculated by the impedance match method based on the measured Us and impact velocity. The shock impedance of antigorite is a little smaller than that of LiF, while their initial densities are very similar each other. LiF has no phase transformation over the pressure range in this study [*Marsh*, 1980]. From the four shots (4, 5, 6, and 1), the factors for Up and pressure in between LiF and antigorite are obtained to be 1.09 and 0.906, respectively. The validity of the factors will be described in next paragraph. Using these factors, the Up and pressure for antigorite were calculated in the other three shots (7, 3 and 2) from the measured Up of LiF, and they are listed as bracketed values in Table 2. The reflected states by the LiF window were calculated by the impedance match methods as

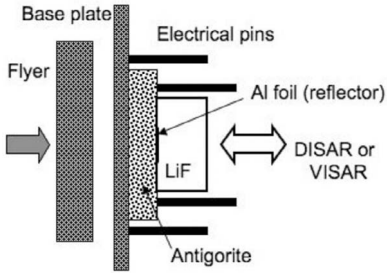

Figure 1. Schematic illustration of target assemblage for measurements of wave profile by planar impact. Flyer was accelerated by a two-stage light gas gun or a propellant gun. Six sets of electrical pins were used to measure the shock velocity by two-stage light gas gun experiments. The particle velocity was measured by DISAR or VISAR (see text). The sample thickness is a range between 2.53 and 2.88 mm. The window of LiF is 8 mm thick.

Table 2. Experimental Conditions and Results on Antigorite and LiF[a]

			LiF			Antigorite				
Shot Number, Density (g/cm^3)	Flyer/Base Plate	Vimp (km/s)	Measured Up (km/s)	Us (km/s)	Pressure (GPa)	Measured Us (km/s)	Calculated Up (km/s)	Pressure (GPa)	Density I (g/cm^3)	Density II (g/cm^3)
7, 2.630	3 mm sus/1 mm sus	1.73(1)	1.22(2)	6.80	21.9	[5.66]	[1.33]	[19.8]	[3.44]	[3.40]
4, 2.626	2.5 mm Al/1.5 mm Al	4.40(2)	2.22(2)	8.15	47.7	6.74(20)	2.44(3)	43.2(8)	4.11(7)	4.29(10)
5, 2.606	2.5 mm Al/1.5 mm Al	4.63(2)	2.30(2)	8.26	50.1	6.80(20)	2.58(3)	45.7(15)	4.20(8)	4.52(10)
6, 2.636	2.5 mm Al/1.5 mm Al	5.47(2)	2.79(2)	8.92	65.7	7.29(30)	3.02(3)	58.1(15)	4.50(13)	4.65(17)
1, 2.643	3 mm Cu/1.5 mm Al	4.18(2)	2.84(4)	8.98	67.4	7.94(32)	2.97(3)	62.2(19)	4.22(10)	4.28(11)
3, 2.623	1.5 mm Ta/0.5 mm Ta	5.34(3)	4.08(5)	10.66	114.8	[8.93]	[4.44]	[104.0]	[5.22]	[4.90]
			2.00(5)	7.85	41.4	-	[2.17]	[37.5]	-	[3.41]
2, 2.638	1.5 mm Ta/0.5 mm Ta	6.31(3)	4.75(5)	11.56	145.0	[9.65]	[5.16]	[131.4]	[5.67]	[5.35]
			2.42(5)	8.42	53.8	-	[2.63]	[48.7]	-	[3.57]

[a]Experimental conditions are initial density of antigorite, flyer and base plate, and impact velocity Vimp. Results are particle velocity Up, shock velocity Us, pressure, and density. Value in parenthesis means error, and one in bracket was calculated using the following factors. Up and pressure for antigorite in shots 7, 3, and 2 are estimated to be 1.09 and 0.906 times of those measured for LiF, respectively (see text for details). The density I is at the Hugoniot state, and density II corresponds to the state recompressed by LiF (first row) or released partially (second row). For the flyer and base plate materials, sus is stainless steel 304, Al is aluminum, Cu copper, and Ta tantalum.

listed in the last column of Table 2. In the two shots 3 and 2, almost flat velocities were observed on the way during pressure release, as shown in Figure 2, and were used to calculate the density of antigorite by the Riemann integral method [*Lyzenga and Ahrens*, 1978], as shown in the second line of shots 3 and 2 in Table 2. Such a temporal flat velocity regime that appeared in shots 3 and 2 after the Hugoniot state corresponds to the state where the induced high-pressure phase is partially released and they exist as mixed phases once a pressure-release wave, originated from the boundary between the flyer and sabot of a projectile, arrives. Its presence implies the phase transition (decomposition) is an irreversible reaction, like in shocked quartz [e.g., *Swegle*, 1990].

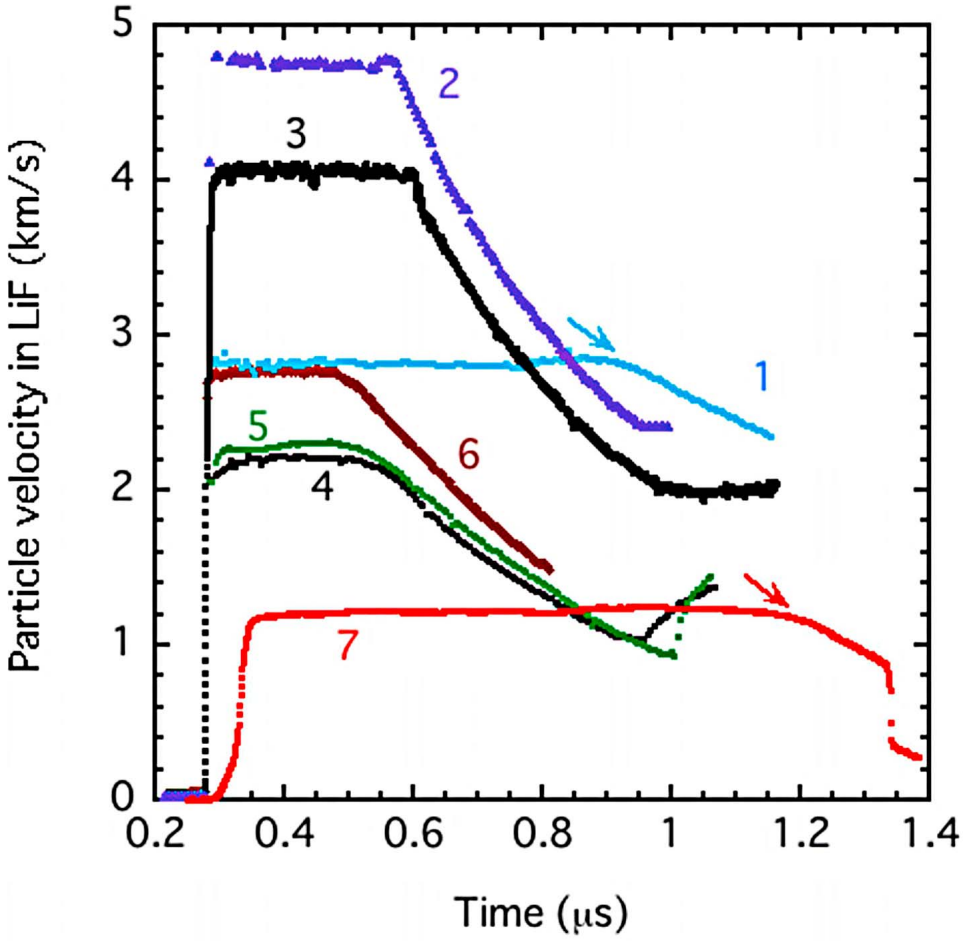

Figure 2. Measured particle velocity profiles. Numbers correspond to the sample number in Table 2, where the detailed experimental conditions are listed together with the analytical results.

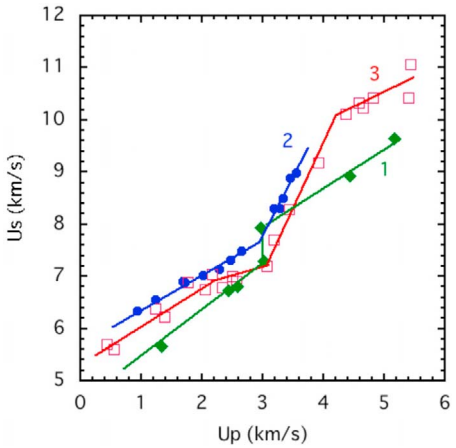

Figure 3. Shock velocity (Us)-particle velocity (Up) relationships for antigorite (solid diamonds, 1) in the present study, serpentinized rock (solid circles, 2) [*Marsh*, 1980], and lizardite (open squares, 3) [*Tyburczy et al.*, 1991].

[9] We describe the validity for the factors to estimate the Up and pressure for antigorite in shots where we did not measure the shock velocity directly. All the measured particle velocities are single wave structure, as shown in Figure 2, and LiF does not have any phase transition. If we refer the lizardite studied by *Tyburczy et al.* [1991] that indicates phase transitions, the P (GPa)-Up (km/s) relation is approximated to be a smooth second-order curve, $P = -0.325 + 13.63Up + 2.549Up^2$ ($R = 0.99345$) up to ~150 GPa. Then P will be approximated by $2.55Up(5.345 + Up)$ at high pressures. Based on these conditions, one can have two equations:

$$P_1 = \rho_{01} Up_1 (C_1 + S_1 Up_1) \text{ for antigorite (initial density of } \rho_{01})$$

$$P_2 = \rho_{02} Up_2 (C_2 + S_2 Up_2) \text{ for LiF (initial density of } \rho_{02})$$

where C_1, S_1, C_2, and S_2 are constants. These two display single shock-wave structures under the experimental condition. We assume; $Up_1 = \alpha Up_2$, $\alpha = 1.09$ and $P_1 = \beta P_2$, $\beta = 0.906$. These α and β are the mean values from the four shots in which both Us and Up were measured experimentally. Then we have

$$P_1/P_2 = (\rho_{01}/\rho_{02})(Up_1/Up_2)(C_1 + S_1 Up_1)/(C_2 + S_2 Up_2).$$

$$(C_1 + S_1 Up_1)/(C_2 + S_2 Up_2) = (\beta/\alpha)(\rho_{02}/\rho_{01}) = \gamma(\approx 0.83)$$

$$Up_1 = (\gamma C_2 - C_1)/S_1 + \gamma(S_2/S_1) Up_2$$

This equation means that Up_1 and Up_2 are linear with constants $(\gamma C_2 - C_1)/S_1$ and $\gamma(S_2/S_1)$ in the present pressure

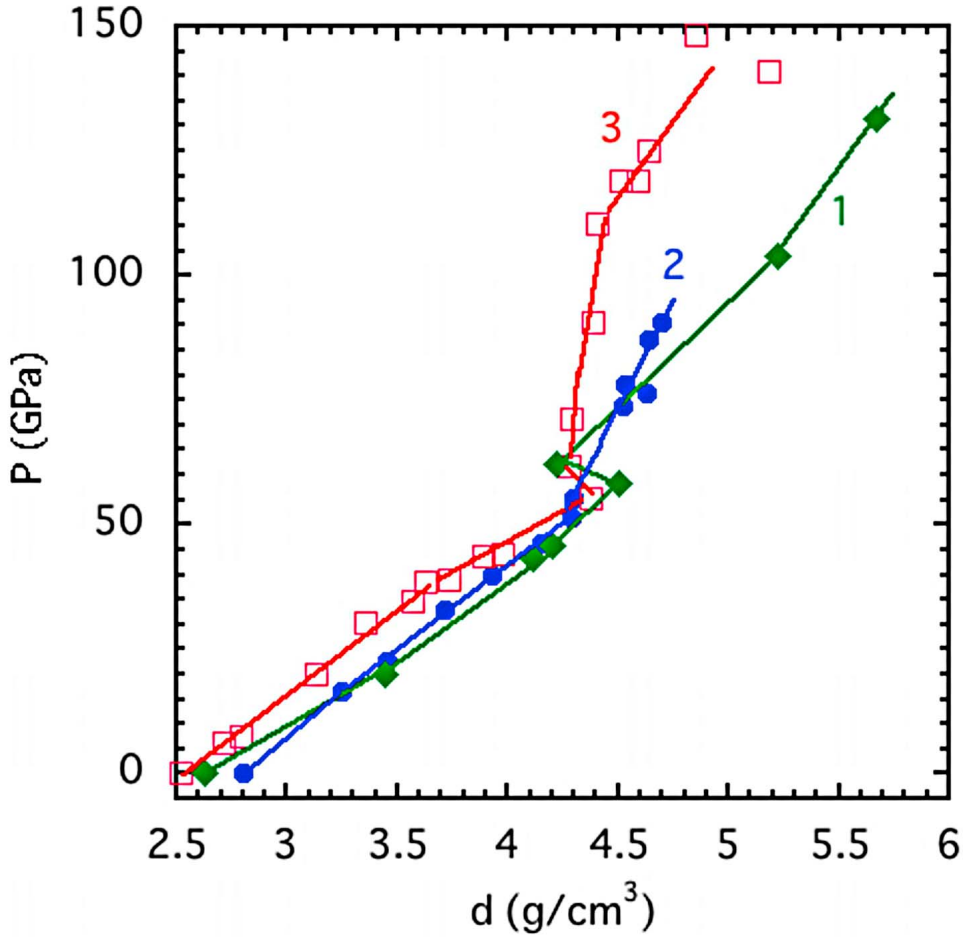

Figure 4. Pressure (P)- density (d) relationships for antigorite (solid diamonds, 1) in the present study, serpentinized rock (solid circles, 2) [*Marsh*, 1980], and lizardite (open squares, 3) [*Tyburczy et al.*, 1991].

range. Here we estimate the constant values based on the data below 60 GPa in Table 2 and the ambient data (Up = 0 and P = 0). If the P-Up relation for antigorite is a second-order curve, P (GPa) is expressed to be 0.0606 + 2.62Up(4.271 + Up) (R = 0.99984) where Up is in km/s. At high pressures, it will be 2.62Up(4.271 + Up). The constants ($\gamma C_2 - C_1)/S_1$ and $\gamma(S_2/S_1)$ are 0.0035 and 1.12, respectively. That means that the value α will not change significantly, being within about 4% of the assumed α value, even if we take a wide range of Up. The value of $\beta = \alpha\gamma(\rho_{01}/\rho_{02})$ also will be within about 4% of the assumed β value. Therefore it is possible to estimate the Up and P for antigorite using the linking factors, α and β, from the measured Up and P for LiF. Thus estimated Up and P values have uncertainties of about 4%, respectively.

[10] Figures 3 and 4 illustrate the relationships between Us and Up and between pressure and density for antigorite to compare with those for lizardite and serpentinised rock. They indicate a change of the Hugoniot compression curve at pressure of around 50 GPa, corresponding to the change around Up = 3 km/s in the Us-Up plots. A density decrease was detected in the present measurements, as shown in Figure 4. A comparison of the Hugoniot compression curves for antigorite and lizardite below ~50 GPa indicates that antigorite is slightly more compressible than lizardite. This behavior is in good agreement with the experimental data of the bulk modulus obtained at static pressures below 10 GPa [*Hilairet et al.*, 2006]. However, these Hugoniot compression curves show a larger divergence above ~60 GPa, as seen in Figure 4.

4. Discussion

[11] The bulk sound velocity and longitudinal velocity of antigorite at ambient condition have been calculated as the Hill, Voigt, and Reuss averages [*Bezacier et al.*, 2010]. If we use the Hill average values, the shock wave travels at the bulk sound velocity and the arrival time difference between the elastic and plastic waves is calculated to be about 0.15 μs at relatively low pressures for the sample thickness (about 3 mm thick). According to the particle velocity profile in shot 7 at the lowest peak shock pressure (~20 GPa), the two-wave structure is not clear but the rising velocity at low pressure (Figure 2, shot 7) indicates a slow velocity increase initially due to such a possible two-wave structure. Figure 3 compares the Us-Up relationship for antigorite, lizardite and serpentinised rock. The present data of Us-Up plot show a similar trend to the previous data of lizardite [*Tyburczy et al.*, 1991] and serpentinized rock [*Marsh*, 1980] up to Up of 3 km/s, but there seems to be a sharp jump around a particle velocity of 3 km/s, where the previous data also indicate a kink at a particle velocity around 3 km/s. Although the present study performed the detailed measurements around the possible phase transition, the present wave profile (Figure 2) did not indicate any evidence for two-wave structure associated with possible phase transformation. Except for the two highest shock pressures, the measured profiles present obvious elasto-plastic transition at the time of initial unloading. At these highest shock pressures, however, the profiles indicate shock-induced softening during unloading and display a reverse transition by the appearance of part of the flat velocity nearly at the end of measurements.

[12] As illustrated in Figure 4, there is a density decrease with increasing pressure about a pressure of 50–60 GPa. Although *Tyburczy et al.* [1991] did not mention this before, their lizardite data also show a similar trend, while it is difficult to see such a trend in the serpentinized rock [*Marsh*, 1980]. In such a pressure region, density decrease with increasing pressure is quite rare in minerals. In low density materials, such behaviors are known due to extremely high temperature effects even below 20 GPa [e.g., *Trunin*, 1998] and it is considered to indicate a large volume expansion associated with the shock compressed material. Such density decrease means (1) abrupt temperature increase or/and (2) large volume expansion during compression. When Fe-free serpentine $Mg_3Si_2O_5(OH)_4$ decomposes into assemblages such as (1) 2 $Mg(OH)_2$ (brucite) + MgO + 2 SiO_2 (stishovite) (the zero-pressure density of 3.14 g/cm^3), (2) 2 $Mg(OH)_2$ (brucite) + $MgSiO_3$ (perovskite) + SiO_2 (stishovite) (the zero-pressure density of 3.17 g/cm^3), and (3) 2 $MgSiO_3$ (perovskite) + MgO + 2 H_2O (the zero-pressure density of 4.00 g/cm^3), theoretical calculations indicate little change in the pressure-density plot [*Tyburczy et al.*, 1991]. Such decompositions, however, are normally exothermic, and they cause temperature increasing in the system to consume the internal energy increase. Enthalpy changes for the three decomposition reactions (1)–(3) at the standard state are 1000.39 kJ/mol, 964.83 kJ/mol, and 378.82 kJ/mol, respectively, if we take data for chrysotile (as serpentine), brucite, periclase, quartz (as stishovite), enstatite (as perovskite), and water [*Robie et al.*, 1979]. When the recompression process in shots 2 and 3 is a decomposition of antigorite, the enthalpy change ΔH can be written by $\Delta H = 0.5(P_2 - P_1)(V_1 + V_2)$ [*Walsh and Rice*, 1957], being 5920 kJ/mol (shot 3) and 6845 kJ/mol (shot 2) based on the values listed in Table 2. These estimations are about six times of the enthalpy change at the standard state. This also may suggest that the decomposition causes greater temperature rises at high shock pressures. Therefore it can be expected larger temperature increase for the decomposition reactions including brucite than the dehydration. Then such a temperature increasing may drop density substantially to keep the system steady. Therefore the observed density drop around 50–60 GPa may indicate an exothermic reaction associated with the decomposition of antigorite. If this is the case, the available Hugoniot data for brucite and muscovite indicate that they will not decompose or be less exothermic at high pressures. The Hugoniot data for topaz $Al_2SiO_4(OH)_2$ [*Simakov et al.*, 1974] also indicate little increase in density at pressure interval between 51 GPa and 65 GPa, although there is no direct data to show a density decrease clearly. This may also imply an exothermic decomposition reaction.

[13] Because decomposition reactions are considered to be fast enough to give a single wave structure normally, the present wave profile could not detect two-wave structure associated with the decomposition [*Rice et al.*, 1958]. The Us-Up plot illustrated in Figure 3 suggests that the two shock wave velocities before and after the decomposition are different, but that the corresponding particle velocities are almost same. After checking carefully the wave profiles of shots 1 with 2–3 times longer duration of compression, a

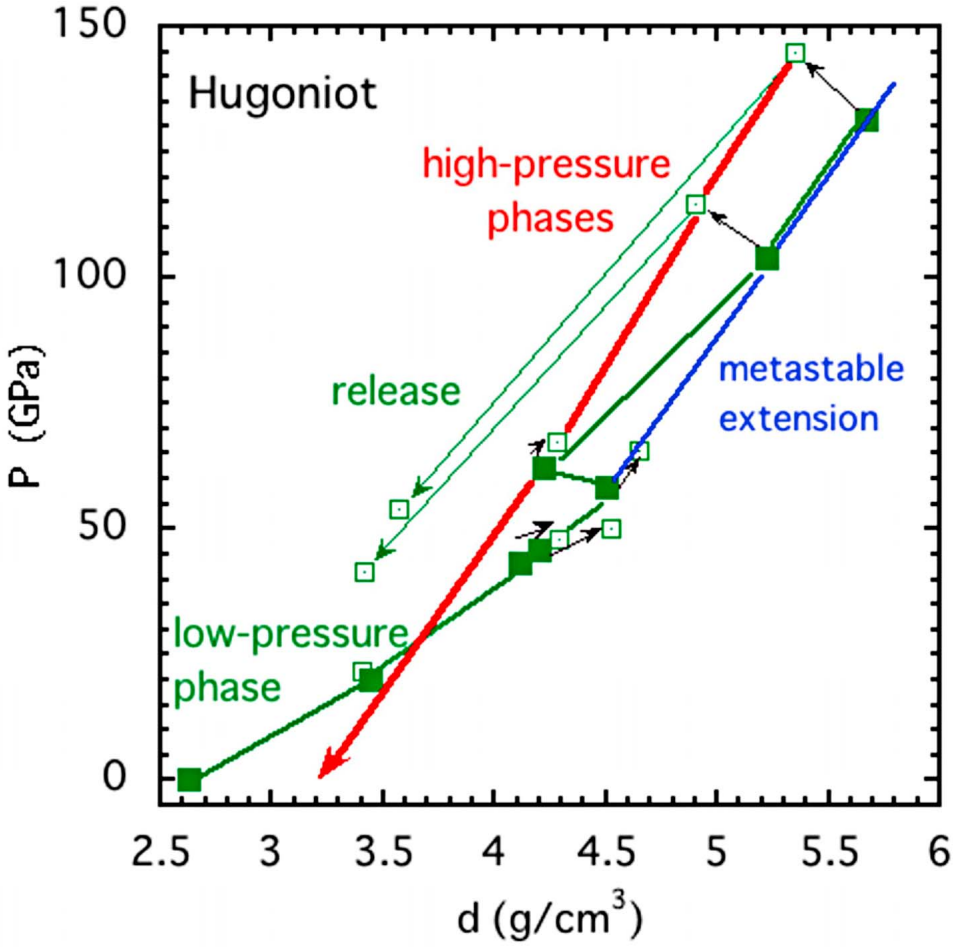

Figure 5. Compression behavior of antigorite and partially released states based on the measured wave profiles. Hugoniot states (solid squares), recompressed states (open squares with short, black arrows), and partially released states (open squares with long arrows). The Hugoniot compression curve for the high-pressure phase, as represented by the recompressed states, is indicted by a heavy line and its extension to zero pressure gives a density of 3.0–3.5 g/cm^3. Arrow shows the direction, but does not indicate the actual path.

dispersion of particle velocity appears at early stage and a slight increase can be seen at a time of 0.9 μs (Figure 2). This may indicate onset of an exothermic decomposition proceeding in this time interval. The wave velocities were measured through the LiF window. LiF has slightly higher shock impedance than the antigorite and recompresses the antigorite a little further by the shock wave reflection. The Hugoniot state before the recompression was estimated from the measured and calculated Us of antigorite and the measured impact velocity by the impedance match solutions. The recompressed states also are calculated based on the measured Up of LiF. Figure 5 gives the change of the recompression and partially released states. The recompression state moves almost along the Hugoniot curve except for shots 3 and 2. In these two shots, densities at the recompressed states decrease a little with increasing pressure. This also may imply exothermic decomposition reactions during the recompression, but not at the Hugoniot states. The Hugoniot states also represent temporal states affected by the kinetic factor when reaction occurs under dynamic conditions. These observations, coupled with the results of shot 1, suggest that the decomposition requires a reaction time for the exothermic reaction.

[14] The shocked states after relatively longer compression at peak pressures may stabilize high-pressure phases. Under such situations, the recompressed states correspond to the states consisting of the stable phases. Taking the compression curve represented by the recompressed states for the high-pressure phases, a rough extension of the curve to zero pressure gives a density about 3.0–3.5 g/cm^3. This is closer to an estimation for the decomposition assemblages of brucite + stishovite + ferrous periclase or brucite + perovskite with zero-pressure densities of 3.14 or 3.17 g/cm^3, rather than that for the dehydration. The released states measured from the two Hugoniot states are plotted in Figure 5. They are located almost parallel to the metastable extension curve in the pressure-density plot and shallower than the slope of the high-pressure phase compression curve. This behavior is in contrast to the results by *Tyburczy et al.* [1991]. Their partially released paths are almost along the Hugoniot compression curve at least in the high-pressure region. We do not know the reason yet, but the decomposition kinetics

may be affected by the state of sample. The chemical composition of the sample used in the present study is very close to that of their sample, but density has about 4% difference.

[15] If serpentine can survive as a metastable phase above the threshold pressure, serpentine may play an important role as a candidate of water carrier during planetary formation because serpentine has greater stability than water ice itself. Due to the high stability, potentially serpentine brings a sufficient amount of water inward the snow line [*van Boekel*, 2007]. In scenarios for planet formation from dust protoplanetary disks, ice condenses when the temperature falls below a certain level called snowline. The present experimental results also imply how water can be carried more effectively than water itself because serpentine persists metastablely to about 60 GPa and because serpentine decomposes into brucite-bearing mineral assembly to keep a significant amount of water in it. The stability of serpentine in a carbonaceous chondrite under dynamic conditions has been investigated in detail [*Akai and Sekine*, 1994; *Tomeoka et al.*, 2003; *Tomioka et al.*, 2007] through the transmission electron microscopic observations of shock-recovered samples. The threshold pressure for the decomposition in such experiments is significantly reduced due to the higher shock temperatures in the porous samples at a pressure even if the samples were subjected to a peak shock pressure achieved by shock reflections. In fact the recovered samples below the threshold peak pressure indicated a gradual decomposition as a function of peak pressure, and the quenched products by the decomposition were amorphous. The final products were recrystallized olivine and low-Ca pyroxene at 30–36 GPa. The glass recovered above a peak pressure of 32 GPa displayed the presence of voids indicating volatile loss during pressure release [*Akai and Sekine*, 1994]. A threshold pressure of 30 GPa corresponds a symmetric impact velocity of 5 km/s in case of Murchison carbonaceous meteorite, which is considered to represent a typical material for asteroids. These shock recovery experimental results clearly indicate that brucite is not the quench product. At ambient state brucite may have been dehydrated due to a high residual temperature before pressure reaches near zero and periclase may have reacted out to disappear. Thermogravimetric analyses for unshocked and shocked Murschison meteorite also indicate H_2O loss as a function of peak shock pressure (22–50 GPa) [*Tyburczy et al.*, 1986], but the estimation of the amount of residual serpentine in the shocked Murschison needs to be checked with the amount of glass which may contain a significant amount of H_2O and other volatiles.

[16] The stability of serpentine depends on not only the time scale of shock compression duration but also how decomposition occurs by shock process. The static high-pressure experiments reveal that the dehydration process of serpentine is slow enough and stepwise depending on the temperature [e.g., *Chollet et al.*, 2011], and also the chemistry and structure of serpentine affect greatly its stability [*Bromiley and Pawley*, 2003]. Coupled with our shock wave experiments indicating possible occurrence of metastable states during shock compression of antigorite, the dehydration process will not be same as the static ones. Further the dehydration products contain brucite as suggested by the present study. It will be also important to address the heterogeneity in meteorite and planetesimal impact process, although the time scale is another key. Actually serpentine can be formed by impact process under water present conditions even in relatively a short time scale [*Furukawa et al.*, 2011]. Therefore, serpentine will become a strong candidate of water carrier in planetary systems [*Lauretta et al.*, 2000; *Ciesla et al.*, 2003; *Brearly*, 2006].

5. Conclusions

[17] Detailed wave profiles of serpentine under shock loading have been measured at pressures up to ~140 GPa by time-resolved methods in order to investigate the phase transition and the dynamic behavior. A clear density decrease with increasing shock pressure was found around 60 GPa when samples were shocked for a longer time and recompressed by reflected shock from the LiF window. This density decrease has been explained by an exothermic decomposition of serpentine into brucite + stishovite + periclase or brucite + perovskite without fluid water. Although shock-induced decompositions are considered to be fast, a time lag has been observed for the decomposition reaction measurable by the time-resolved wave profiles in the present study. High metastability of serpentine and its decomposition products at pressures above 60 GPa under shock loading may have played a key role to carry water inward the snowline during the planetary formation process through the collisional accretions.

[18] **Acknowledgments.** The authors are grateful to the technical staff of the National Key Laboratory of Shock Wave and Detonation Physics (LSD), Institute of Fluid Physics, CAEP, China, for their help with the plate impact experiments. The collaboration of T.S. with LSD was supported by the Foundation of National Key Laboratory of shock wave and Detonation Physics 9140C670203110C6705. Experiment in NIMS, Japan, was done while T.S. was there. We are thankful for the reviewers' comments and suggestions to improve the draft.

References

Akai, J., and T. Sekine (1994), Shock effects experiments on serpentine and thermal metamorphic conditions in Antarctic carbonaceous chondrite, *Proc. NIPR Symp. Antarct. Meteorites*, *7*, 101–109.

Barker, L. M., and R. E. Hollenbach (1972), Laser interferometer for measuring high velocities of any reflector, *J. Appl. Phys.*, *43*, 4669–4675, doi:10.1063/1.1660986.

Bezacier, L., B. Raynard, J. D. Bass, C. Sanchez-Valle, and B. Van de Moortèle (2010), Elasticity of antigorite, seismic detection of serpentines, and anisotropy in subduction zones, *Earth Planet. Sci. Lett.*, *289*, 198–208, doi:10.1016/j.epsl.2009.11.009.

Brearly, A. J. (2006), The accretion of water, in *Meteorites and the Early Solar Systems II*, edited by D. S. Lauretta and H. Y. McSween Jr., pp. 587–624, Univ. Ariz. Press, Tucson.

Bromiley, G. D., and A. R. Pawley (2003), The stability of antigorite in the systems $MgO\text{-}SiO_2\text{-}H_2O$ (MSH) and $MgO\text{-}Al_2O_3\text{-}SiO_2\text{-}H_2O$ (MASH): The effects of Al^{3+} substitution on high-pressure stability, *Am. Mineral.*, *88*, 99–108.

Chollet, M., I. Danniel, K. T. Koga, G. Morard, and B. van de Moortèle (2011), Kinetics and mechanism of antigorite dehydration: Implications for subducted zone seismicity, *J. Geophys. Res.*, *116*, B04203, doi:10.1029/2010JB007739.

Christensen, N. I. (2004), Serpentines, peridotites, and seismology, *Int. Geol. Rev.*, *46*, 795–816, doi:10.2747/0020-6814.46.9.795.

Ciesla, F. J., D. S. Lauretta, B. A. Cohen, and L. L. Hood (2003), A nebular origin for chondritic fine-grained phyllosilicates, *Science*, *299*, 549–552, doi:10.1126/science.1079427.

Dobson, D. P., P. G. Meredith, and S. A. Boon (2002), Simulation of subduction zone seismicity by dehydration of serpentine, *Science*, *298*, 1407–1410, doi:10.1126/science.1075390.

Duffy, T. S., T. J. Ahrens, and M. A. Lange (1991), The shock wave equation of state of brucite $Mg(OH)_2$, *J. Geophys. Res.*, *96*, 14,319–14,330, doi:10.1029/91JB00987.

Furukawa, Y., T. Sekine, T. Kakegawa, and H. Nakazawa (2011), Impact-induced phyllosilicate formation from olivine and water, *Geochim. Cosmochim. Acta*, *75*, 6461–6472, doi:10.1016/j.gca.2011.08.029.

Hilairet, N., I. Daniel, and B. Reynard (2006), P-V equations of state and the relative stabilities of serpentine varieties, *Phys. Chem. Miner.*, *33*, 629–637, doi:10.1007/s00269-006-0111-0.

Irifune, T., K. Kuroda, N. Funamori, T. Uchida, T. Yagi, T. Inoue, and N. Miyajima (1996), Amorphization of serpentine at high pressure and high temperature, *Science*, *272*, 1468–1470, doi:10.1126/science.272.5267.1468.

Jensen, B. J., D. B. Holtkam, P. A. Rigg, and D. H. Dolan (2007), Accuracy limits and window corrections for photon Doppler velocimetry, *J. Appl. Phys.*, *101*, 013523, doi:10.1063/1.2407290.

Jung, H. Y., Y. W. Fei, P. G. Silver, and H. W. Green II (2009), Frictional sliding in serpentine at very high pressure, *Earth Planet. Sci. Lett.*, *277*, 273–279, doi:10.1016/j.epsl.2008.10.019.

Katayama, I., K. Hirauchi, K. Michibayashi, and J. Ando (2009), Trench-parallel anisotropy produced by serpentine deformation in the hydrated mantle wedge, *Nature*, *461*, 1114–1117, doi:10.1038/nature08513.

Lauretta, D. S., X. Hua, and P. R. Buseck (2000), Mineralogy of fine-grained rims in the ALH 81002 CM chondrite, *Geochim. Cosmochim. Acta*, *64*, 3263–3273, doi:10.1016/S0016-7037(00)00425-7.

Lyzenga, G. A., and T. J. Ahrens (1978), The relation between the shock-induced free-surface velocity and the postshock specific volume of solids, *J. Appl. Phys.*, *49*, 201–204, doi:10.1063/1.324323.

Marsh, S. P. (Ed.) (1980), *LASL Shock Hugoniot Data*, Univ. of Calif. Press, Berkeley.

Mookherjee, M., and L. Stixrude (2009), Structure and elasticity of serpentine at high-pressure, *Earth Planet. Sci. Lett.*, *279*, 11–19, doi:10.1016/j.epsl.2008.12.018.

Rice, M. H., R. G. McQueen, and J. M. Walsh (1958), Compression of solids by strong shock waves, *Solid State Phys.*, *6*, 1–63, doi:10.1016/S0081-1947(08)60724-9.

Robie, R. A., B. S. Hemingway, and J. R. Fisher (1979), Thermodynamic properties of minerals and related substances at 298.15 K and 1 bar (10^5 Pascals) pressure and at higher temperatures, *Bull. 1452*, U.S. Geol. Surv., Washington, D. C.

Schmitt, D. R., Z. Han, V. A. Kravchinsky, and J. Escartin (2007), Seismic and magnetic anisotropy of serpentinized ophiolite: Implications for oceanic spreading rate dependent anisotropy, *Earth Planet. Sci. Lett.*, *261*, 590–601, doi:10.1016/j.epsl.2007.07.024.

Sekine, T., A. M. Rubin, and T. J. Ahrens (1991), Shock equation of state of muscovite, *J. Geophys. Res.*, *96*, 19,675–19,680, doi:10.1029/91JB02253.

Sekine, T., T. Kobayashi, M. Nishio, and E. Takahashi (2008), Shock equation of state of basalt, *Earth Planets Space*, *60*, 999–1003.

Simakov, G. V., M. N. Pavlovskiy, N. G. Kalashnikov, and R. F. Trunin (1974), Shock compressibility of twelve minerals, *Phys. Solid Earth*, *8*, 11–17.

Stalder, R., and P. Ulmer (2001), Phase relations of a serpentine composition between 5 and 14 GPa: Significance of clinohumite and phase E as water carriers into the transition zone, *Contrib. Mineral. Petrol.*, *140*, 670–679, doi:10.1007/s004100000208.

Swegle, J. W. (1990), Irreversible phase transition and wave propagation in silicate materials, *J. Appl. Phys.*, *68*, 1563–1579, doi:10.1063/1.346635.

Tomeoka, K., K. Kuriyama, K. Nakamura, Y. Yamahana, and T. Sekine (2003), Interplanetary dust from explosive dispersal of hydrated asteroids by impacts, *Nature*, *423*, 60–62, doi:10.1038/nature01567.

Tomioka, N., K. Tomeoka, K. Nakamura-Messenger, and T. Sekine (2007), Heating effects of the matrix of experimentally shocked Murchison CM chondrite; Comparison with micrometeorites, *Meteorit. Planet. Sci.*, *42*, 19–30, doi:10.1111/j.1945-5100.2007.tb00214.x.

Trunin, R. F. (1998), *Shock Compression of Condensed Materials*, Cambridge Univ. Press, Cambridge, U. K., doi:10.1017/CBO9780511599835.

Tyburczy, J. A., B. Frich, and T. J. Ahrens (1986), Shock-induced volatile loss from a carbonaceous chondrite: Implications for planetary accretion, *Earth Planet. Sci. Lett.*, *80*, 201–207, doi:10.1016/0012-821X(86)90104-4.

Tyburczy, J. A., T. S. Duffy, T. J. Ahrens, and M. A. Lange (1991), Shock wave equation of state of serpentine to 150 GPa: Implications for the occurrence of water in the Earth lower mantle, *J. Geophys. Res.*, *96*, 18,011–18,027, doi:10.1029/91JB01573.

Uehara, S., and H. Shirozu (1985), Variations in chemical composition and structural properties of antigorites, *Mineral. J.*, *12*, 299–318, doi:10.2465/minerj.12.299.

van Boekel, R. (2007), Water worlds in the making, *Nature*, *447*, 535–536, doi:10.1038/447535a.

Walsh, J. M., and M. H. Rice (1957), Dynamic compression of liquids from measurements on strong shock waves, *J. Chem. Phys.*, *26*, 815–823, doi:10.1063/1.1743414.

Weng, J. D., H. Tan, X. Wang, Y. Ma, S. L. Hu, and X. S. Wang (2006), Optical-fiber interferometer for velocity measurements with picosecond resolution, *Appl. Phys. Lett.*, *89*, 111101, doi:10.1063/1.2335948.

Weng, J. D., X. Wang, Y. Ma, H. Tan, L. C. Cai, J. F. Li, and C. L. Liu (2008), A compact all-fiber displacement interferometer for measuring the foil velocity driven by laser, *Rev. Sci. Instrum.*, *79*, 113101, doi:10.1063/1.3020700.

H. He, C. Meng, and W. Zhu, National Key Laboratory of Shock Wave and Detonation Physics, Institute of Fluid Physics, Chinese Academy of Engineering Physics, PO Box 919-111, Mianyang, Sichuan 621900, China.

T. Sekine, Department of Earth and Planetary Systems Science, Hiroshima University, Kagamiyama 1-3-1, Higashi-Hiroshima 739-8526, Japan. (toshimori-sekine@hiroshima-u.ac.jp)